

## Physical properties of 3D and 2D Ruddlesden-Popper halide perovskite semiconductors

J. Even<sup>\*1</sup>, H. Tsai<sup>2</sup>, W. Nie<sup>2</sup>, J.-C. Blancon<sup>2</sup>, A. Neukirch<sup>2</sup>, L. Pedesseau<sup>1</sup>, S. Boyer-Richard<sup>1</sup>, B. Traoré<sup>3</sup>, M. Kepenekian<sup>3</sup>, J.-M. Jancu<sup>1</sup>, C. Stoumpos<sup>4</sup>, S. Tretiak<sup>2</sup>, M. Kanatzidis<sup>4</sup>, A. Mohite<sup>2</sup>, and C. Katan<sup>3</sup>

<sup>1</sup> FOTON, UMR 6082, CNRS, INSA Rennes, Rennes, France

<sup>2</sup> Los Alamos National Laboratory, Los Alamos, New Mexico, USA

<sup>3</sup> ISCR, UMR 6226, CNRS, Université de Rennes 1, Rennes, France

<sup>4</sup> Department of Chemistry, Northwestern University, Evanston, Illinois USA

In the past five years, solution-processed organometallic perovskite based solar cells have emerged as a promising thin-film photovoltaic technology. Presently, the intended optoelectronic applications of this class of materials are in the realm of conventional semiconductors. Meanwhile, in this new family of semiconductors, the spin-orbit coupling is giant and shows up in the conduction band, the band gap is direct with the critical wavevector located at one of the edges of the reference Brillouin zone, and all these distinctive features deserve a specific theoretical framework.<sup>1</sup> Then, the electronic band structure can be modeled using either Density Functional Theory calculations or empirical methods such as the tight-binding model and the multiband **k.p** method.<sup>2</sup> Among others, excitonic effects play a crucial role in ensuring device efficiencies. For instance, in 3D halide-based hybrid perovskites, the strong reduction of the exciton binding energy at room temperature is essential for the operation of photovoltaic devices.<sup>1,3</sup> Related 2D Ruddlesden-Popper phases, composed of perovskites layers sandwiched between two layers of large organic cations, have recently demonstrated improved photostability under standard illumination as well as humidity resistance over 2000 hours, affording a conversion efficiency of 12.5 %.<sup>4</sup> In this case, intrinsic quantum<sup>5</sup> and dielectric carrier confinements<sup>6</sup> are afforded by the organic inner barriers, which leads to a stable Wannier exciton at room temperature.

### References

<sup>1</sup> J. Even et al, Phys. Rev. B 2012, J.Phys. Chem Lett. 2013, J. Phys. Chem. C 2014

<sup>2</sup> J. Even et al, Rapid Research Lett. 2014, S. Boyer-Richard, J. Phys. Chem. Lett. 2016

<sup>3</sup> H.H. Fang et al, Adv. Func. Mat. 2015, W. Nie et al, Nature Comm. 2016

<sup>4</sup> H. Tsai et al, Nature 2016

<sup>5</sup> J. Even et al, ChemPhysChem 2014, J. Phys. Chem. Lett. 2015

<sup>6</sup> D. Saporì et al, Nanoscale 2016, L. Pedesseau et al, ACS Nano 2016

The project leading to this application has received funding from the European Union's Horizon 2020 programme, through a FET Open research and innovation action under grant agreement No 687008.

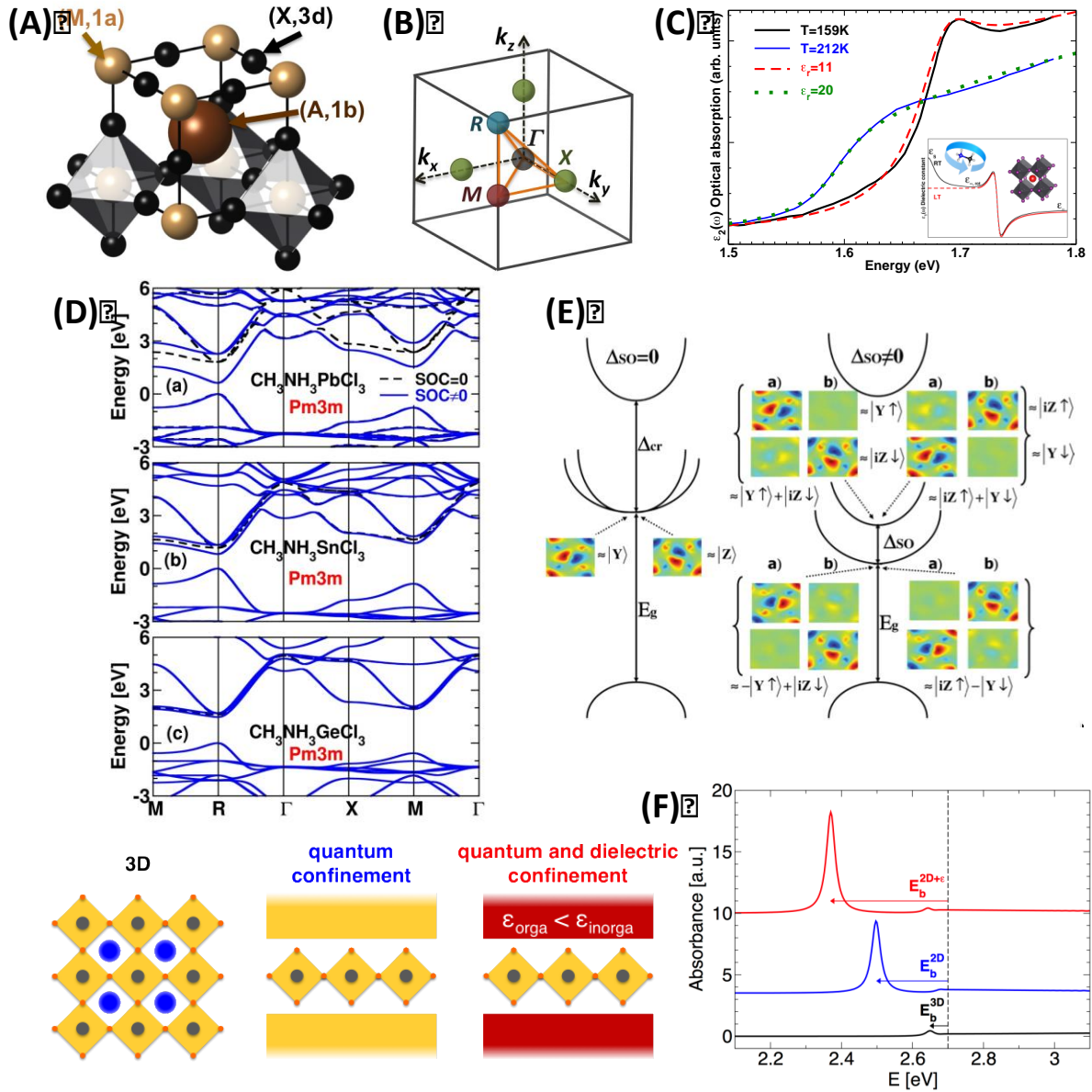


Fig. 1. (A) Real space 3D view of the  $Pm\bar{3}m$  reference cubic crystal structure of metal-halide perovskites of general formulae  $AMX_3$  where A is an inorganic or an organic cation, M a metal and X an halogen. (B) Reciprocal space 3D view showing the first Brillouin Zone (BZ) of the  $Pm\bar{3}m$  space group. Points of high symmetry in the cubic BZ are indicated by conventional letters with  $\Gamma$  denoting the origin of the BZ; X the center of a square face,  $M(1/2,1/2,0)$  a center of a cube edge and  $R(1/2,1/2,1/2)$  a vertex of the cube. (C) Optical absorption spectra of  $CH_3NH_3PbI_3$  highlighting exciton screening. Experimental data recorded at 159 K (black line) and 212 K (blue line) are taken from T. Ishihara, J. of Lum. 1994, 60&61, 269. Theoretical spectra for bound and continuum pair states are computed considering two-particle wave function and effective mass equations for electron and hole. (D) Electronic band diagrams for the high temperature cubic phases ( $Pm\bar{3}m$ ) of  $CH_3NH_3MX_3$ : (a)  $M=Pb$  (b)  $M=Sn$  and (c)  $M=Ge$ , calculated at the LDA level of theory without (black dashed lines) and with (blue straight lines) Spin Orbit Coupling (SOC). (E) Schematic representation the electronic band diagram without ( $\Delta_{SO}=0$ ) and with ( $\Delta_{SO}\neq 0$ ) the SOC interaction.  $\Delta_{cr}$  represents the anisotropy of the crystal field and  $E_g$  the band gap energy. The real (a) and imaginary (b) parts of the complex spinorial components of the CBM1 and CBM2 states are represented for the 2D hybrid perovskite  $[pFC_6H_5C_2H_4NH_3]_2PbI_4$ , with the spin up component plotted on top of the spin down component. (F) Optical absorption computed using a  $\mathbf{k}\cdot\mathbf{p}$ /BSE approach for a model hybrid perovskite considered as a 3D material with  $\epsilon_{\infty} = 5.0$  (black line), a 2D material with only quantum confinement and  $\epsilon_{\infty} = 5.0$  (blue line), a 2D material with both quantum and dielectric confinement (red line).